Multidimensional CP-MAS 13C NMR of uniformly enriched chlorophyll

Rossum, B.-J. van; Boender, G.-J; Mulder, F.M.; Raap, J.; Balaban, T.S.; Holzwarth, A.R.; ... ; Groot, H.J.M. de

ELSEVIER

Spectrochimica Acta Part A 54 (1998) 1167–1176

SPECTROCHIMICA ACTA PART A

Multidimensional CP-MAS ^{13}C NMR of uniformly enriched chlorophyll

B.-J. van Rossum [a,*], G.J. Boender [a], F.M. Mulder [a], J. Raap [a], T.S. Balaban [b], A. Holzwarth [b], K. Schaffner [b], S. Prytulla [c], H. Oschkinat [c], H.J.M. de Groot [a]

[a] *Leiden Institute of Chemistry, Gorlaeus Laboratories, P.O. Box 9502, 2300 RA Leiden, The Netherlands*
[b] *Max-Planck Institut für Strahlenchemie, Stiftstraße, D-45470 Mülheim a/d Ruhr, Germany*
[c] *EMBL, P.O. Box 10.2209, D-69117 Heidelberg, Germany*

Abstract

The progress toward structure refinement of solid-type uniformly ^{13}C enriched ([U-^{13}C]) chlorophyll-containing biological preparations is summarised. Solid state carbon chemical shifts of aggregated [U-^{13}C] bacteriochlorophyll (BChl) *c* in intact chlorosomes of *Chlorobium tepidum* and in [U-^{13}C] BChl *c* aggregates were determined by the application of homonuclear (^{13}C–^{13}C) magic angle spinning (MAS) NMR dipolar correlation spectroscopy. It was found that the arrangement of BChl *c* molecules in the chlorosomes and in the aggregates is highly similar, which provides convincing evidence that self-organisation of the BChl *c* is the main mechanism to support the structure of the chlorosomes. Additionally, high field 2-D (^{1}H–^{13}C) and 3-D (^{1}H–^{13}C–^{13}C) dipolar correlation spectroscopy was applied to determine solid state proton chemical shifts of aggregated [U-^{13}C] BChl *c* in intact chlorosomes. From the high-field assignments, evidence is found for the existence of at least two well-defined interstack arrangements.

Keywords: Antenna; Photosynthesis; MAS NMR; Isotope labelling; Chlorophyll

1. CP/MAS NMR spectroscopy of photosynthetic components

In recent years, progress has been made in forging pathways for obtaining magic angle spinning (MAS) NMR access to photosynthetic components [1]. These studies rely on the use of labeling schemes and ^{13}C cross-polarisation (CP) MAS NMR. The natural abundance of ^{13}C is low, and in order to enhance the sensitivity, the use of ^{13}C enriched biological samples is a prerequisite. For instance, using labeled spheroidene obtained

Abbreviations: BChl *c*, bacteriochlorophyll *c*; Chl *a*, chlorophyll *a*; CIDNP, chemically induced dynamic nuclear polarisation; COSY, correlated spectroscopy; CP, cross-polarisation; FSLG, frequency-switched Lee-Goldburg; MAS, magic angle spinning; NMR, nuclear magnetic resonance; RC, reaction centre; Q_A, primary quinone acceptor; RFDR, radio frequency-driven dipolar recoupling; TPPM, two pulse phase-modulation; U-^{13}C, uniformly ^{13}C enriched; WISE, wideline separation.

* Corresponding author. Tel.: +31 71 5274539; fax: +31 71 5274603; e-mail: ssnmr@chem.leidenuniv.nl

1386-1425/98/$19.00
PII S1386-1425(98)00067-5

by total synthesis, the configuration of the 15–15′ bond of the carotenoid reconstituted into the R26 reaction centre (RC) was characterised [2]. In addition, the electronic ground state of the primary quinone acceptor (Q_A) in the reaction centre has been probed with MAS NMR and isotope labeling [3]. An advantage of selective labeling of cofactors is a direct and straightforward chemical shift assignment of the response from the nucleus of interest. However, selective labeling is most often difficult to realise. In particular for chlorophyll, to arrive at a complete set of specifically labeled molecules at every individual position would probably take decades of organic synthesis work.

Recently, different routes for obtaining information from multiply enriched samples were explored. For instance, the details of the electronic ground state structure of the RC protein-complex of *Rhodobacter sphaeroides* have been investigated for tyrosine side chains labeled at the 4′-position, with particular focus on M210 and L162, that are of importance for the efficiency of the charge separation and re-reduction processes in the RC [4–6]. In these studies, all tyrosines in the RC were selectively labeled, and assignment of the two specific residues, M210 and L162, was done by illumination or mutation [4–6]. In another approach, a novel example of photochemically induced dynamic nuclear polarisation (photo-CIDNP) was discovered, yielding strong emissive signals for Q_A depleted, or pre-reduced uniformly ^{15}N labeled RCs [7]. The first assignments for a multi-spin cluster in a large protein complex using NMR dipolar correlation spectroscopy were obtained recently for RCs of *Rhodobacter sphaeroides*, reconstituted with [U-^{13}C] pheophytin *a* [8]. Finally, it was found that the large chemical shift dispersion of the ^{13}C response of ~ 200 ppm can be exploited for high-resolution dipolar correlation spectroscopy of ^{13}C nuclei in multiply enriched samples, due to the truncation of the homonuclear dipolar interactions by the chemical shift dispersion in high magnetic fields. This yields remarkably narrow lines in the 2-D ^{13}C–^{13}C dipolar correlation spectra of uniformly enriched chlorophylls [9].

The specific aim of this review is to summarise progress toward assignment strategies and structure refinement of large solid-type uniformly ^{13}C enriched chlorophyll-containing biological preparations [9–11]. Recently, MAS NMR dipolar correlation spectroscopy was used to provide a characterisation at the molecular level of the structure of an intact chlorosome photosynthetic antenna system that is inaccessible to X-ray or solution NMR approaches [10,11]. The resolution that can be achieved with homonuclear (^{13}C–^{13}C) dipolar correlation spectroscopy offers promising possibilities for a further development of assignment strategies and concepts for structural characterisation of biomolecules in steps.

The dipolar correlation methods rely on the re-introduction of dipolar interactions by multi-pulse recoupling sequences. Several pulse techniques are now available for restoring homonuclear dipolar interactions between ^{13}C nuclei in a MAS experiment [12–18]. A first concept for structure refinement is starting to emerge, and is schematically depicted in Fig. 1 [19]. Using a multiply labeled sample, homonuclear and heteronuclear correlation spectra are recorded, in two or three dimensions. Subsequently, the spectra are analysed to obtain an assignment of the chemical shifts. From the homonuclear (^{13}C–^{13}C) dipolar correlation spectra, the assignment of the carbon resonances is first obtained. The carbon assignment is used to assign the proton chemical shifts in 2-D (^{1}H–^{13}C) or 3-D (^{1}H–^{13}C–^{13}C) heteronuclear correlation spectra. Since ^{13}C shifts are generally quite sensitive to atomic charge density variations, the shifts provide information about

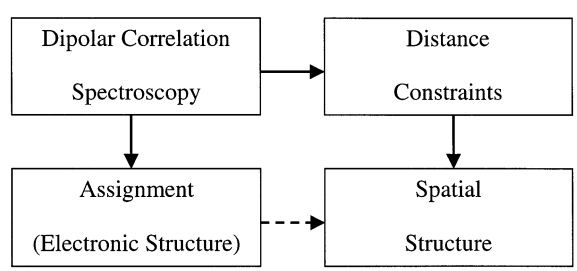

Fig. 1. A possible concept for structure refinement with multi-dimensional MAS NMR dipolar correlation spectroscopy (schematic).

the electronic structure of the molecule at the atomic level. In an interpretation step, indicated with the dashed arrow in Fig. 1, the knowledge about the electronic structure can help to model a spatial structure. Independently, dipolar correlation spectra can provide 'hard' structural restraints from intermolecular correlations that can be used to refine the modeling, as indicated by the solid arrows [19].

^{1}H NMR in solids is notoriously difficult due to the combination of the very strong homonuclear dipolar interactions between the abundant protons and of the small chemical shift dispersion of protons. A good resolution can be obtained by ^{13}C detection and by exploiting the large ^{13}C chemical shift dispersion in heteronuclear (^{1}H–^{13}C) correlation spectroscopy. For instance, it was demonstrated that straightforward high-speed MAS heteronuclear (^{1}H–^{13}C) cross-polarisation wide-line separation (CP/WISE) spectroscopy performed in a high magnetic field and without any homonuclear decoupling scheme during the proton evolution yields resolved ^{1}H–^{13}C correlations and proton shift assignments [20,21]. Additional resolution enhancement can be achieved by adding a third dimension. When the heteronuclear CP/WISE is combined with homonuclear broadband radio frequency-driven dipolar recoupling (RFDR) correlation spectroscopy in a high magnetic field, 3-D spectra are obtained with sufficient resolution in the proton dimension to assign the observed proton resonances of moderately sized molecules or multispin clusters [22].

2. MAS NMR investigations of ^{13}C-enriched chlorosomes and aggregates

An interesting example of a chlorophyll based photosynthetic component is found in a chlorosome antenna system. Chlorosomes are oblong bodies attached to the inner side of the cytoplasmic membrane [23,24]. A variety of experimental data obtained over the last decade has provided converging evidence that in the chlorosomes a distinctive organisational principle for an antenna system seems to be realised, based on self-organisation of BChl not directly mediated by proteins [25,26]. Crystallisation of chlorosome-type aggregates was not yet accomplished and therefore diffraction techniques cannot be used to study the structure at the atomic level. In contrast, information on both the spatial and the electronic structure of the micro-crystalline chlorophyll in the chlorosome assemblies can be acquired with solid state NMR spectroscopy [10].

2.1. ^{13}C MAS NMR evidence for highly similar arrangement of BChl c in chlorosomes and in the aggregated form

It is known that BChl *c* forms aggregates both in non-polar [27,28] and in aqueous media [29]. The long wavelength absorption of native chlorosomes (740–750 nm) can be reproduced with BChl *c* aggregates in non-polar solvents [27]. In Fig. 2, the contour plots of 2-D homonuclear (^{13}C–^{13}C) dipolar correlation spectra of [U-^{13}C] BChl *c* in the chlorosomes (Fig. 2A) and of the [U-^{13}C] BChl *c* in the in vitro aggregates (Fig. 2B) are shown. These spectra were obtained with the RFDR pulse sequence [9,13]. The signals forming the diagonals in the spectra correspond with the 1-D NMR response of the ^{13}C nuclei in the sample. The characteristic MAS sideband lines parallel to the diagonal are present at integral multiples of the spinning speed and are clearly visible. Abundant cross-peaks reveal polarisation transfer between ^{13}C nuclei.

The 2-D dipolar correlation spectra of the chlorosomes and the BChl *c* aggregates are strikingly similar, and it is evident that most of the ^{13}C response from the chlorosome is associated with BChl *c*. This provides direct and unambiguous spectral evidence that BChl *c* is the major component of the chlorosomes [10]. In addition, the ^{13}C line-widths for corresponding carbon sites in the spectra of the chlorosomes compare very well with those for the aggregates and also for the cross-peaks.

The widths of the BChl *c* response for both samples are roughly twice the line-widths observed for the resonances of [U-^{13}C] chlorophyll *a* aggregates [9]. This may reflect structural or electronic disorder or incommensurability. Chlorosomes of *Chlorobium tepidum* contain at least five

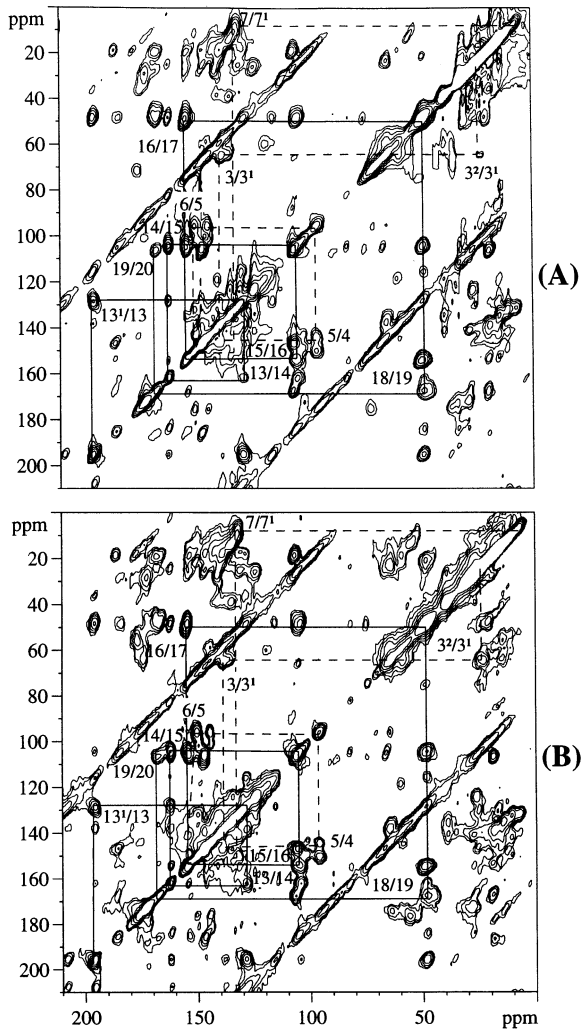

Fig. 2. Contour plots of 2-D MAS dipolar correlation NMR spectra of uniformly ^{13}C labeled chlorosomes (A), and ^{13}C labeled bacteriochlorophyll *c* aggregates (B), recorded in a magnetic field of 9.4 T. The spinning speed was 8. kHz and a polarisation transfer time of 1 ms was used. The lines indicate sequences of nearest neighbour correlations. The assignments of correlations (*x*/*y*) on the plot correspond with the numbering of the bacteriochlorophyll *c* in Fig. 5.

BChl *c* homologues [10]. However, the presence of different homologues of BChl *c* cannot explain the inhomogeneous line broadening, since the ^{13}C line-widths in the spectrum of aggregates prepared from only one [U-^{13}C] BChl *c* homolog are approximately the same as observed for the BChl *c* mixtures [10,19]. In the contour plot in Fig. 2A only few signals appear that are not present in the spectrum of the in vitro aggregates. These could be assigned to a small protein fraction and to the lipids of the chlorosomes [10,19].

To assign the ^{13}C response of BChl *c*, RFDR spectra with a mixing time of 1 ms and with various spinning speeds were collected from [U-^{13}C] chlorosomes and the in vitro [U-^{13}C] BChl *c* aggregates. The resolution of the set of 2-D spectra is sufficient to allow the identification of a large number of individual correlations and to arrive at a complete assignment of the ^{13}C response [10]. The relatively short mixing time ensures that the observed cross-peaks in these spectra are predominantly associated with nearest-neighbour carbon-carbon correlations. The lines in Fig. 2 connecting cross-peaks and diagonal peaks illustrate how the molecular ^{13}C framework gives rise to a correlation network. From the assignment it can be concluded that the chemical shifts of BChl *c* in the chlorosomes and in the aggregated form are identical within the experimental error [10]. This strongly suggests that the arrangement of BChl *c* molecules in the chlorosomes and in the aggregates is highly similar, which provides convincing evidence that self-organisation of the BChl *c* is the main mechanism to support the structure of the chlorosomes. It confirms an early hypothesis that the in vitro aggregates are good models for the in vivo chlorosomal structure [30].

In addition to the ^{13}C shifts, ^{1}H shifts will be invaluable for structure refinement of the BChl *c* stack. Considerable proton aggregation shifts can be expected, for instance due to ring-currents in the chlorin macrocycles or polarisation effects in the region of binding moieties. It has been demonstrated that high magnetic fields attenuate the ^{1}H homonuclear dipolar line broadening to such an extent that signals in a MAS 2-D heteronuclear correlation spectrum can be resolved [21]. A 2-D heteronuclear (^{1}H–^{13}C) CP/WISE correlation spectrum was recorded from the [U-^{13}C] BChl *c* chlorosomes in a magnetic field of 14.1 T (Fig. 3). The ^{1}H signals correlated with the olefinic ^{13}C are resolved and can be assigned. On the other hand, there is strong overlap between aliphatic protons in the 2-D data. With the improved resolution of

a 3-D heteronuclear (^{1}H–^{13}C–^{13}C) correlation spectrum an assignment of all observable ^{1}H resonances can be obtained [22].

In the heteronuclear correlation spectra the 5-CH and the 7^1-CH_3 responses are divided over two sets of signals. The strongest 5-C response has $\sigma_i = 95.1$ ppm, correlated with an ^{1}H signal with $\sigma_i = 8.3$ ppm, while a weaker fraction is observed that has $\sigma_i = 101.2$ ppm for the ^{13}C and $\sigma_i = 7.4$ ppm for the ^{1}H. Although the 5-C response with $\sigma_i = 101.2$ ppm is close to the shift in solution, it is unlikely that this signal arises from free BChl *c* in the chlorosome sample, since the correlated proton response is shifted upfield more than 2 ppm with respect to the 5-H proton of monomeric BChl *c*. The major part of the 7^1-C response is found at $\sigma_i = 10.4$ ppm and correlates with protons having $\sigma_i = 3.0$ ppm, while a weaker 7^1-C response has $\sigma_i = 6.6$ ppm for the ^{13}C with $\sigma_i = -0.5$ ppm for the correlated protons.

The division of signals over two fractions was not resolved in the 2-D ^{13}C spectra of Fig. 2 that were collected with a ^{13}C frequency of 100 MHz [10]. In the same manner as the protons, increasing the magnetic field strength enhances the resolution for the ^{13}C. The presence of two fractions could be resolved by a 150 MHz homonuclear

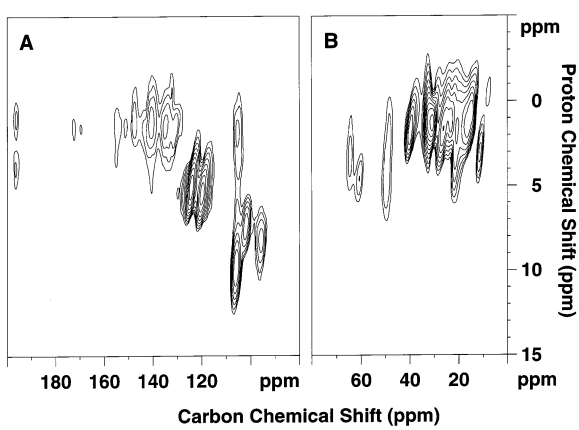

Fig. 3. Contour plots of the ^{13}C olefinic (A) and ^{13}C aliphatic (B) regions of a 2-D MAS heteronuclear (^{1}H–^{13}C) dipolar correlation spectrum of uniformly ^{13}C enriched chlorosomes collected in a magnetic field of 14.1 T. A spinning speed of 15. kHz was used and the cross-polarisation contact time was 250 μs. The correlation spectrum was recorded without ^{1}H homonuclear decoupling.

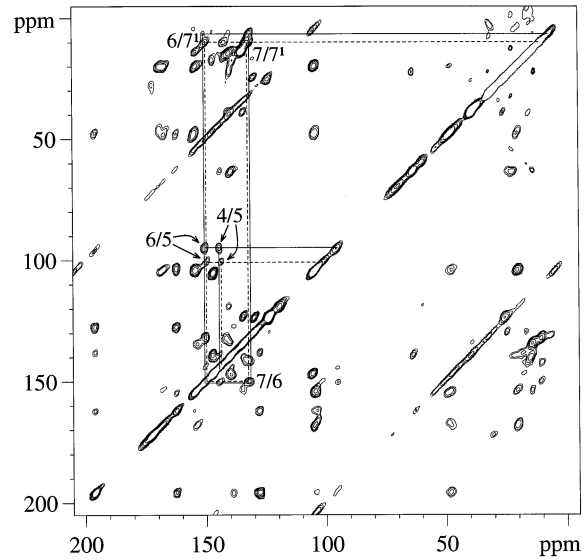

Fig. 4. Contour plot of a 2-D MAS ^{13}C–^{13}C dipolar correlation NMR spectrum of uniformly ^{13}C enriched chlorosomes collected in a magnetic field of 14.1 T. The spectrum was recorded with a spinning speed of 15. kHz and with a polarisation transfer time of 1 ms. The solid and dashed lines indicate the correlation networks 4-5-6-7-7^1 for the two components.

^{13}C–^{13}C RFDR spectrum of the [U-^{13}C] BChl *c* chlorosomes (Fig. 4). This emphasises the need for high fields when performing multidimensional MAS dipolar correlation spectroscopy of uniformly enriched biological samples.

The solid lines in Fig. 4 indicate the correlation network 4-5-6-7-7^1 that includes the strongest response from the 5-C at 95.1 ppm and the 7^1-C response at 6.6 ppm. The next-nearest neighbour correlation between the 6-C and the 7^1-C was crucial to close the correlation network. For the other fraction, indicated by the dashed lines, the correlations between the 5-C at 101.2 ppm and minor 4-C and 6-C responses at 143.5 and 149.8 ppm, respectively, are well resolved. In addition, cross peaks between the 7-C and 7^1-C, and between the 6-C and 7^1-C have been assigned.

2.2. The stacking of BChl c in chlorosomes

As pointed out schematically in Fig. 1 with dashed arrow, an interpretation of the chemical shifts can be of assistance in the development of a

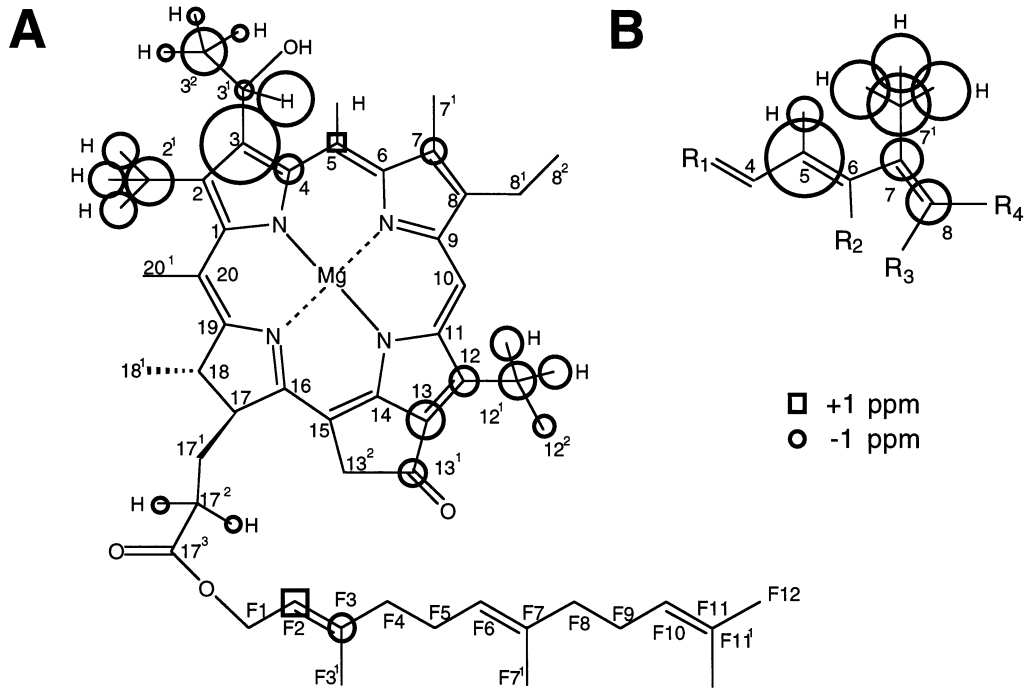

Fig. 5. Visual representation of the aggregation shifts $\Delta\sigma_i = \sigma_{liq} - \sigma_i$. The two components shown in Fig. 4 by the solid and dashed lines are indicated separately in (A) and (B).

NMR structural model for the stacking of BChl *c* in the chlorosomes. To this end, carbon aggregation shifts $\Delta\sigma_i$ were calculated for the datasets in Figs. 2 and 4 [10,19]. For every carbon position its $\Delta\sigma_i$ is defined as the difference between the shift in the aggregate and the shift in a monomer, i.e. in solution. This leads to the translation of the NMR data in Fig. 2 into a semi-quantitative picture of the interactions of the molecule with its immediate surroundings. In Fig. 5 the aggregation shifts are plotted on the chemical structure of the BChl *c*, for the carbons with $|\Delta\sigma_i| \geq 1$ ppm. The circles around the carbon atoms represent upfield aggregation shifts, while the squares correspond with downfield $\Delta\sigma_i$. The size of a sphere or square is proportional to the magnitude of the aggregation shift. The larger $|\Delta\sigma_i| > 2$ ppm are detected for 2^1-C (-3.0 ppm), 3-C (-5 ppm), 3^2-C (-2.8 ppm), 5-C (-5 ppm), 7-C (-2.5 ppm), 7^1-C (-4 ppm), 8-C (-3 ppm), 12^1-C (-2.3 ppm) and 13-C (-2.4 ppm).

As for the ^{13}C, it is possible to define proton aggregation shifts $\Delta\sigma_i$ relative to the shifts measured for the ^{1}H response of monomeric BChl *c* in solution. These aggregation shifts are also visualised in Fig. 5 for $|\Delta\sigma_i| \geq 1$ ppm. Circles around hydrogen atoms correspond with upfield aggregation shifts. Proton aggregation shifts $|\Delta\sigma_i| \geq 1$ ppm are detected for 5-CH (1.3 and 2.2 ppm), 3^1-CH (3.3 ppm), 3^2-CH_3 (1 ppm), 2^1-CH_3 (2.2 ppm), 12^1-CH_2 (2 ppm), 7^1-CH_3 (3.7 ppm) and 17^2-CH_2 (1 ppm) [22].

The carbon aggregation shifts were used in the process of modelling the stacking of the BChl *c* [11]. It was inferred that the stacking in the BChl *c* aggregates should follow the stacking in the parallel chain model shown in Fig. 6 [11,31]. The proton aggregation shifts of the 3^1-CH, 3^2-CH_3, 2^1-CH_3, and 12^1-CH_2 (Fig. 5A) confirm that the region of the 3 side chain, the 2^1-methyl, and the region around the 12-C and 13-C are affected by the aggregation process. This is well in line with the ^{13}C results [10,19] and supports the model for the stack (Fig. 6). In addition, the NMR is already discriminative at this semi-quantitative level, since the ring overlap model, which predicts

large ring-current shifts that are not observed in the NMR, was rejected [10,32].

The carbon aggregation shifts for the 4-, 5- and 7-C of the first component are visualised in Fig. 5A. Likewise, Fig. 5B shows the carbon aggregation shifts for the 5-, 7-, 7^1-C and 8-C, and the proton aggregation shifts for the 5-H and 7^1-H_3 of the other component. The distribution of the NMR response over two signals appears to be restricted to one corner of the molecule. The large upfield proton aggregation shifts of -3.7 ppm for the 7^1-H_3 are intriguing. Interestingly, the 7^1-protons are not much affected by e.g. ring current shifts for all BChl *c* model species that could be studied in solution [33,34]. It is tempting to conclude that the upfield aggregation shifts observed for part of the 7^1-Me response in the chlorosomes are an indication that at least two well-defined interstack arrangements exist, for instance due to ends of stacks in contact with the side of neighbouring stacks, which may be necessary to form the rod-like suprastructure in the chlorosomes.

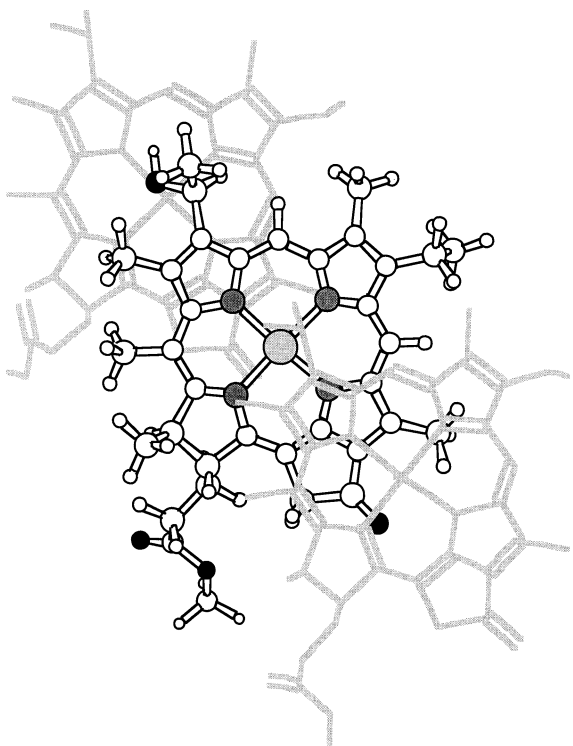

Fig. 6. Schematic representation of the putative molecular arrangement of bacteriochlorophyll *c* in the chlorosomes [31]. In the centre, the ball-and-stick representation was used to highlight a macro-aromatic ring of bacteriochlorophyll *c*. The macro-aromatic rings of two neighbouring bacteriochlorophyll *c* molecules in the stack are represented with grey wire-frames for clarity.

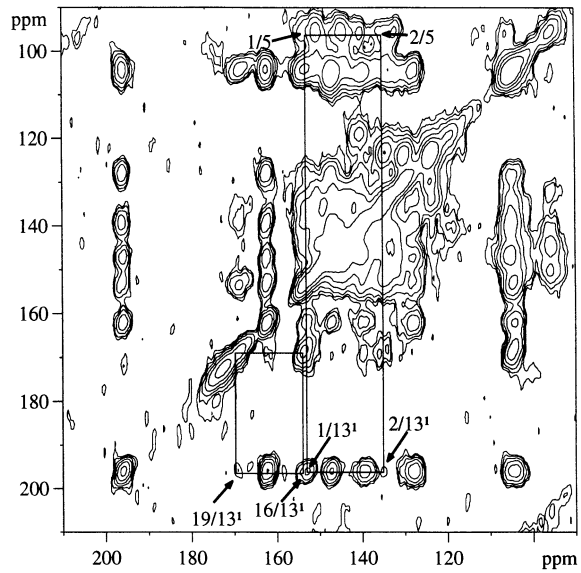

Fig. 7. Selection of a contour plot of a 2-D MAS dipolar correlation NMR spectrum of uniformly ^{13}C-labeled chlorosomes, collected in a magnetic field of 9.4 T. The spinning speed was 11. kHz and the polarisation transfer time was ~ 10 ms. The correlations are indicated by vertical or horizontal lines and with arrows.

When RFDR spectra are recorded with relatively long mixing times (5–10 ms), relayed polarisation transfer can proceed over several adjacent nuclei [19]. This is illustrated with the 2-D correlation spectrum collected with a mixing time of ~ 10 ms from the [U-^{13}C] chlorosomes, shown in Fig. 7. For instance, the 13^1-C, resonating at 195.8 ppm, strongly correlates with its nearest neighbour at position 13 (127.9 ppm), and also with the 12-C (139 ppm), 14-C (162.1 ppm), 15-C (104.3 ppm), and 16-C (153.6) [19]. In addition, weak transfer from the 13^1-C to the 19-C (168.1 ppm), 20-C (105.0 ppm), 1-C (153.2 ppm), 2-C (135.2 ppm) and 3-C (139 ppm) at the opposite side of the molecule was reported [19]. The correlations with 19-C, 20-C, 1-C, 2-C and 3-C were attributed to intermolecular transfer. In terms of

the schematic picture of Fig. 1, this leads to the distance constraints that appear to confirm the low resolution model for the stacking of the chlorophyll in the chlorosome and in the aggregate via the direct route indicated by the solid arrows [19]. It should be stressed, however, that the intermolecular transfer is in competition with intramolecular relayed polarisation transfer in the relatively small chlorophyll ring system. The relayed spin diffusion was briefly investigated for [U-^{13}C] tyrosine, and it was reported to be limited to five adjacent nuclei in this particular case [19].

3. Future outlook

In the preceding sections we have sketched a global concept for structure determination following the scheme in Fig. 1, based on multispin labeling and multidimensional MAS NMR.

Encouraging progress has been made in enhancing the resolution of homonuclear and heteronuclear dipolar correlation spectra. 2-D ^{13}C spectra can now be recorded from well-ordered samples with excellent resolution. This is illustrated with Fig. 8, which shows a homonuclear dipolar correlation spectrum recorded with the RFDR technique from uniformly ^{13}C enriched chlorophyll *a* aggregates. The resolution in this ^{13}C spectrum compares well with the typical resolution obtained for 2-D proton NMR in solution. The data were acquired in a high static magnetic field, using a high spinning speed and the efficient two pulse phase-modulation (TPPM) proton decoupling technique [35], while the sample was placed in the centre of the NMR-coil with spacers in the rotor.

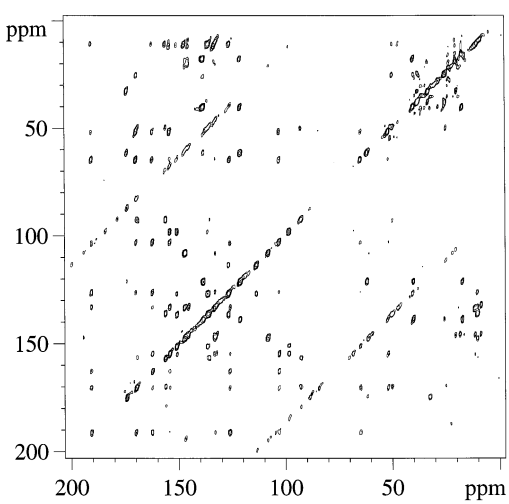

Fig. 8. Contour plot of a 2-D MAS ^{13}C–^{13}C dipolar correlation spectrum of uniformly ^{13}C enriched chlorophyll *a* aggregates, collected in a magnetic field of 14.1 T. A spinning speed of 13. kHz and a polarisation transfer time of 2.46 ms were used.

In high-field MAS experiments, high spinning speeds are required to obtain sufficient resolution in the multidimensional spectra. For fast MAS heteronuclear (^{1}H–^{13}C) correlation spectroscopy, the resolution on the proton side in can be improved dramatically through the application of frequency-switched Lee-Goldburg (FSLG) irradiation during the proton evolution [36]. The basic concept of the Lee-Goldburg experiment is to achieve homonuclear ^{1}H decoupling by the application of an off-resonance RF field in such a way that the effective field in the rotating frame is inclined at the magic angle with respect to the static field in the z-direction [37]. Due to the short Lee-Goldburg cycle time of typically 10 μs, the FSLG irradiation performs well even at high spinning speeds, in contrast to most other techniques that combine MAS with multipulse sequences to suppress the homonuclear dipolar interaction between protons [36].

In Fig. 9 we present a high-field and high-spinning speed 2-D heteronuclear FSLG decoupled correlation spectrum from [U-^{13}C] chlorophyll *a* aggregates. The data were recorded using a modified version of the pulse sequence discussed in Ref. [36]. The sequence starts with a 90° x-pulse. This preparation pulse puts the magnetisation along y, which is perpendicular to the direction of the effective field during the Lee-Goldburg irradiation. In the modified pulse sequence (Fig. 10), the phase of the preparation pulse is cycled between $+x$ and $-x$. The additional phase cycling is necessary to suppress a spin-lock artefact that builds up during the FSLG irradiation. The 2-D heteronuclear dipolar correlation spectrum shown in Fig. 9 is essentially free of artefacts in the entire range of proton reso-

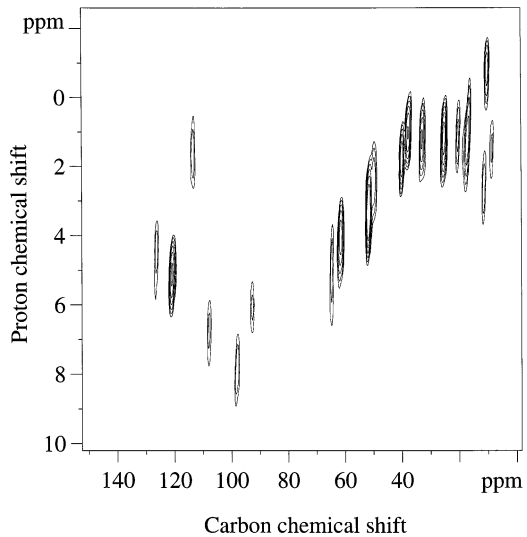

Fig. 9. Heteronuclear (^{1}H–^{13}C) frequency-switched Lee-Goldburg decoupled correlation spectrum from uniformly ^{13}C labeled chlorophyll *a* aggregates, recorded in a magnetic field of 14.1 T and with a spinning speed of 13. kHz.

nances. The overall resolution is good, even for the aliphatic protons.

Heteronuclear dipolar correlation spectroscopy using FSLG homonuclear decoupling is a promising tool for the assignment of proton resonances in biological samples. The strong homonuclear dipolar interactions between protons can provide efficient polarisation transfer pathways, as new pulse sequences will come along. Therefore, it is anticipated that more refined concepts for MAS NMR structure determination will be established in the very near future.

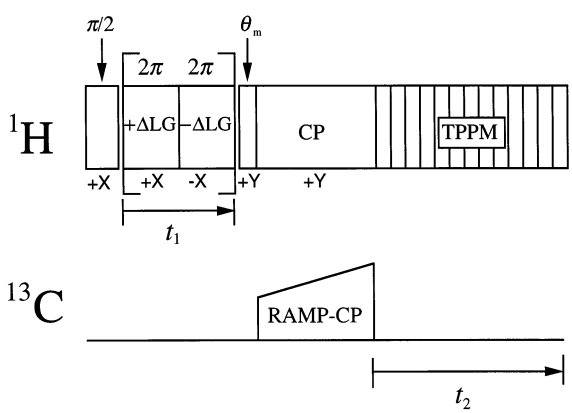

Fig. 10. Pulse sequence for the 2-D heteronuclear correlation spectra with frequency-switched Lee-Goldburg irradiation during the proton evolution.

Acknowledgements

We wish to thank C. Erkelens for support during various stages of the work and E. Schulten for assistance handling the [U-^{13}C] chlorophyll *a* sample. Bruker is gratefully acknowledged for the loan of a high-field CP/MAS probe. This research was financed in part by Demonstration Project Exploratory Award BIO4-CT95-9048 of the European Commission.

References

[1] H.J.M. de Groot, Biophysical techniques in photosynthesis, in: J. Amesz, A.J. Hoff (Eds.), Advances in Photosynthesis, vol. 3, Kluwer, Dordrecht, 1996, pp. 299–313.
[2] H.J.M. de Groot, G. Gebhard, I. vd Hoef, A.J. Hoff, J. Lugtenburg, C.A. Violette, H.A. Frank, Biochemistry 31 (1992) 12446.
[3] W.B.S. van Liemt, G.J. Boender, P. Gast, A.J. Hoff, J. Lugtenburg, H.J.M. de Groot, Biochemistry 34 (1995) 10229.
[4] M.R. Fischer, H.J.M. de Groot, J. Raap, C. Winkel, A.J. Hoff, J. Lugtenburg, Biochemistry 31 (1992) 11038.
[5] S. Shochat, P. Gast, A.J. Hoff, G.J. Boender, S. van Leeuwen, W.B.S. van Liemt, E. Vijgenboom, J. Raap, J. Lugtenburg, H.J.M. de Groot, Spectrochim. Acta A51 (1995) 135.
[6] B.-J. van Rossum, J. Wachtveitl, J. Raap, K. v.d. Hoeff, P. Gast, J. Lugtenburg, D. Oesterhelt, H.J.M. de Groot, Spectrochim. Acta A53 (1997) 2201.
[7] M. Zysmilich, A.E. McDermott, J. Am. Chem. Soc. 116 (1994) 8362.
[8] T.A. Egorova-Zachernyuk, B. van Rossum, G.J. Boender, E. Franken, J. Ashurst, J. Raap, P. Gast, A.J. Hoff, H. Oschkinat, H.J.M. de Groot, Biochemistry 36 (1997) 7513.
[9] G.J. Boender, J. Raap, S. Prytulla, H. Oschkinat, H.J.M. de Groot, Chem. Phys. Lett. 237 (1995) 502.
[10] T.S. Balaban, A.R. Holzwarth, K. Schaffner, G.-J. Boender, H.J.M. de Groot, Biochemistry 34 (1995) 15259.
[11] G.J. Boender, T.S. Balaban, A.R. Holtzwarth, K. Schaffner, J. Raap, S. Prytulla, H. Oschkinat and H.J.M. de Groot, in: P. Mathis (ed.) Photosynthesis: From Light to Biosphere, vol. 1, 1995, p. 347.
[12] D.P. Raleigh, M.H. Levitt, R.G. Griffin, Chem. Phys. Lett. 146 (1988) 71.

[13] A.E. Bennett, J.H. Ok, R.G. Griffin, S. Vega, J. Chem. Phys. 96 (1992) 8642.
[14] T. Gullion, S. Vega, Chem. Phys. Lett. 194 (1992) 423.
[15] T. Fujiwara, A. Ramamoorthy, K. Nagayama, K. Hioka, T. Fujito, Chem. Phys. Lett. 212 (1993) 81.
[16] M. Baldus, M. Tomaselli, B.H. Meier, R.R. Ernst, Chem. Phys. Lett. 230 (1994) 329.
[17] B.-Q. Sun, P.R. Costa, D. Kocisko, P.T. Lansbury, R.G. Griffin, J. Chem. Phys. 102 (1994) 702.
[18] Y.K. Lee, N.D. Kurur, M. Helmle, O.G. Johannessen, N.C. Nielsen, M.H. Levitt, Chem. Phys. Lett. 242 (1995) 304.
[19] G.J. Boender, Ph.D. thesis, University of Leiden, Leiden, The Netherlands, 1996.
[20] K. Schmidt-Rohr, J. Clauss, H.W. Spiess, Macromolecules 25 (1992) 3273.
[21] B.-J. van Rossum, G.J. Boender, H.J.M. de Groot, J. Magn. Reson. A 120 (1996) 274.
[22] B.-J. van Rossum, F.M. Mulder, G.J. Boender and H.J.M. de Groot, T.S. Balaban, A.R. Holzwarth and K. Schaffner, (1997) in preparation.
[23] L.A. Staehelin, J.R. Golecki, R.C. Fuller, G. Drews, Arch. Mikrobiol. 119 (1978) 269.
[24] L.A. Staehelin, J.R. Golecki, G. Drews, Biochim. Biophys. Acta 589 (1980) 30.
[25] A.R. Holzwarth, K. Griebenow, K.Z. Schaffner, Z. Naturforsch. 45C (1990) 203.
[26] A.R. Holzwarth, K. Griebenow, K.J. Schaffner, J. Photochem. Photobiol. A 65 (1992) 61.
[27] M.I. Bystrova, I.N. Mal'gosheva, A.A. Krasnovskii, Mol. Biol. Engl. Trans. 13 (1979) 440.
[28] K.M. Smith, L.A. Kehres, J. Fajer, J. Am. Chem. Soc. 105 (1983) 1387.
[29] M. Miller, T. Gillbro, J.M. Olson, Photochem. Photobiol. 57 (1993) 98.
[30] D.L. Worcester, T.J. Michalski, J.J. Katz, Proc. Natl. Acad. Sci. USA 83 (1986) 3791.
[31] A.R. Holtzwarth, K. Schaffner, Photosyn. Res. 41 (1994) 225.
[32] T. Nozawa, K. Ohtomo, M. Suzuki, H. Nakagawa, Y. Shikama, H. Konami, Z.-Y. Wang, Photosyn. Res. 41 (1994) 211.
[33] T. Mizoguchi, L. Limantara, K. Matsuura, K. Shimada, Y. Koyama, J. Mol. Struct. 379 (1996) 249.
[34] T. Mizoguchi, K. Matsuura, K. Shimada, Y. Koyama, Chem. Phys. Lett. 260 (1996) 153.
[35] A.E. Bennet, C.M. Rienstra, M. Auger, K.V. Lakshmi, R.G. Griffin, J. Chem. Phys. 1023 (1995) 6951.
[36] B.-J. van Rossum, H. Förster, H.J.M. de Groot, J. Magn. Reson. 124 (1997) 516.
[37] M. Lee, W.I. Goldburg, Phys. Rev. A140 (1965) 1261.